

1

## 2 **Supplementary Information for**

### 3 **All-electrical monitoring of bacterial antibiotic susceptibility in a microfluidic device**

4 **Yichao Yang, Kalpana Gupta, and Kamil L. Ekinci**

5 **Kamil L. Ekinci.**  
6 **E-mail: [ekinci@bu.edu](mailto:ekinci@bu.edu)**

#### 7 **This PDF file includes:**

- 8     Supplementary text
- 9     Figs. S1 to S6
- 10    Tables S1 to S4
- 11    Captions for Movies S1 to S2
- 12    References for SI reference citations

#### 13 **Other supplementary materials for this manuscript include the following:**

- 14     Movies S1 to S2

## 15 Supporting Information Text

### 16 Supplemental Materials and Methods

17 **Device Design and Fabrication.** In designing the device, we used a first-pass optimization to determine the number  $k$  of parallel  
18 microchannels. The throughput increases (and the loading time decreases) with increasing  $k$ . However, the available signal  
19 from a microchannel is divided between  $k$  parallel resistors (see the resistance change calculation due to a single bacterium  
20 below). The use of  $k = 10$  parallel microchannels allowed us to achieve a loading time  $\lesssim 30$  min and to comfortably observe  
21 resistance changes due to single cells.

22 Molds for the two-layer microfluidic channel are fabricated by patterning SU-8 photoresist (Microchem, Newton, MA) onto  
23 a 4-inch silicon wafer. After mixing pre-polymer with cross-linker (Sylgard 184, Dow Corning, Midland, MI) at a 9:1 ratio, the  
24 mixture is degassed in a vacuum desiccator for 30 minutes. Next, the bubble free PDMS mixture is slowly poured onto the SU-8  
25 mold and cured in a 90°C oven for 1 hour. The slab of PDMS with the embedded two-layer microfluidic channel structure is  
26 carefully peeled off from the master. Inlet and outlet ports (0.75 mm diameter) are mechanically punched into the PDMS using  
27 a biopsy punch. The PDMS structure and a glass slide with pre-defined metallic electrodes are sterilized and bonded through  
28 oxygen plasma treatment. To fabricate the chromium (Cr) and gold (Au) electrodes onto the glass slide, we use electron beam  
29 evaporation. The electrodes are fabricated by evaporating a 90-nm-thick Au layer on top of a 60-nm-thick Cr adhesion layer.

30 **Bacteria Culturing.** First, lyophilized bacteria are re-solubilized and mixed gently with 1 mL of LB broth, and the solution  
31 is transferred into 5 mL of LB broth for each bacterial strain. Next, the bacteria are grown in a shaking incubator at 37°C  
32 and 100 rpm for 24 hours. After 24 hours, the turbid bacterial suspension is centrifuged for 6 minutes at 6000 rpm, and the  
33 bacteria pellet is re-suspended in 5 mL of fresh LB broth. Finally, frozen stocks are prepared by dissolving highly purified  
34 glycerol (MP Biomedicals, Solon, OH) at 20% v/v in PBS (Lonza BioWhittaker, Walkersville, MD), mixing with bacterial  
35 suspension at 1:1 ratio, collecting into 200  $\mu$ L aliquots and storing at  $-80^\circ\text{C}$ . On the day prior to the experiment, a frozen  
36 stock is thawed, of which 150  $\mu$ L is transferred into 8 mL of fresh LB broth; 10  $\mu$ L of the bacterial culture is streaked on  
37 a LB agar (Becton Dickinson, Sparks Glencoe, MD) plate and grown overnight to check the purity of the bacterial culture.  
38 Bacteria are cultured overnight at 37°C in a shaking incubator at 100 rpm. On the day of the experiment, the bacteria culture  
39 is diluted to the desired concentration. We measure the optical density of the culture at a wavelength of 600 nm ( $\text{OD}_{600}$ ) using  
40 a spectrophotometer (V-1200, VWR, Radnor, PA). An  $\text{OD}_{600}$  of 0.1 corresponds to a bacterial cell density of  $2 \times 10^7$  CFU/mL,  
41 which is periodically confirmed through serial dilution plating on LB agar plates.

42 **Resazurin-Based Broth Microdilution AST.** In order to compare our method with standard methods, the susceptibility of *E.*  
43 *coli*, *K. pneumoniae*, and *S. saprophyticus* are determined using resazurin-based broth microdilution AST standardized by the  
44 Clinical and Laboratory Standard Institute (CLSI). To ensure consistency, *E. coli* (ATCC 25922), for which the MICs of both  
45 ampicillin and nalidixic acid are 4 mg/L (1), is used as a reference strain for all the resazurin-based microdilution tests. First,  
46 ampicillin and nalidixic acid are diluted from stock solutions in LB broth. Column 12 of the 96-well plate is used as growth  
47 control (no antibiotics); column 11 is used as sterility control (no bacteria); and columns 1-10 are filled with solutions with  
48 decreasing antibiotic concentrations, which are prepared by using the two-fold serial dilution method. Next, the bacterial  
49 cultures are prepared separately at 37°C in 8 mL of LB broth. After adjusting their  $\text{OD}_{600}$  to 0.1, the solution is further  
50 diluted by a factor of 20 with LB broth. Then, 100  $\mu$ L of bacteria solution is added to each well of columns 1 to 10, and  
51 column 12. The final bacterial concentration in each well is  $5 \times 10^5$  CFU/mL. The bacterial suspensions are used within 30 min  
52 after their optical density are adjusted to avoid changes of cell numbers (2). Each concentration is replicated in three wells in  
53 each plate. After incubating the plate at 37°C in a shaking incubator at 100 rpm for 16-20 hours, 60  $\mu$ L 0.015% solution of  
54 resazurin (ACROS Organics, New Jersey, USA) in tissue culture grade water is added to each well and further incubated at  
55 37°C for another 4 hours. The plate results are read by visual inspection of the wells. Dark blue/purple indicates that bacteria  
56 are not viable, and pink indicates that bacteria are still viable. If the growth control shows dark blue/purple or the sterility  
57 control indicates contamination, the plate is discarded. The MICs determined using the resazurin-based broth microdilution  
58 AST are summarized in Table S1.

59 **Experimental Protocol for Electrical Measurements.** We measure the growth of *E. coli*, *K. pneumoniae*, and *S. saprophyticus* in  
60 LB broth with and without antibiotics. After adjusting an overnight bacterial culture to an  $\text{OD}_{600}$  of 0.1, the culture is diluted  
61 1:20 into 5 mL LB broth and, depending on the experiment, mixed with antibiotics in equal volume. This results in a final  
62 bacterial cell density of  $5 \times 10^5$  CFU/mL. The mixture is transferred into a sterile 15-mL Falcon tube that is used as a sample  
63 reservoir. A fluorinated ethylene propylene (FEP) tube (Cole-Parmer, Vernon Hills, IL) is used to connect the sample reservoir  
64 to the microfluidic device inlet. During sample loading, the inlet is pressurized at  $\Delta p \sim 10$  kPa above the outlet. The number  
65 of trapped bacteria is typically not uniform across microchannels. After approximately tens of bacteria are trapped in the  
66 microchannels, voltage drop across the microchannels is measured to quantify the bacterial growth. During the measurements,  
67 the pressure difference between inlet and outlet is maintained at  $\Delta p \sim 0.5$  kPa. The pressure during loading is controlled using  
68 a pressure controller (OB1-Mk3, Elveflow, Paris, France). To ensure a stable temperature of the microfluidic device during an  
69 experiment, a PeCon 2000-2 Temp Controller (PeCon GmbH, Erbach, Germany) is used. To show that our microfluidic device  
70 can be used to determine MICs for antibiotics in human urine samples, we measure *K. pneumoniae* in nalidixic acid and *E. coli*  
71 (non-motile) in ampicillin. Bacteria concentration is adjusted to an  $\text{OD}_{600}$  of 0.1, and the bacteria solution is diluted 1:20 in 5

72 mL of human urine sample. Subsequently, the bacteria-spiked urine samples are mixed with LB broth and nalidixic acid (0, 4,  
73 8, 16, and 32 mg/L) or ampicillin (0, 2, 4, 8, and 16 mg/L) in equal volume prior to loading into a microfluidic device.

74 **Electrical Measurements.** Fig. S1 shows the simplified equivalent circuit model of the electrical measurement. The lock-in  
75 amplifier oscillator output  $V_s$  (rms amplitude of 1 V and reference frequency of  $f_r = 10$  Hz) is connected to a resistor  
76  $R_s = 100$  M $\Omega$  to create a current source, which drives a current (several nA) through the device and the input circuit of the  
77 lock-in. The input resistance of the lock-in amplifier is 10 M $\Omega$ . We use a four-wire measurement to measure the resistance  
78 of the device. At  $f_r = 10$  Hz, the four-wire electrical impedance of the device is dominated by its resistance; typical device  
79 impedance at the start of each experiment is  $\approx 3 - 0.2i$  M $\Omega$ , corresponding to a phase angle of  $-4^\circ$ . The resistance value  
80 and the phase both drift over the course of two hours. The drift in the resistance is  $\lesssim 1\%$  and the impedance phase angle is  
81  $\pm 1^\circ$ . We estimate each contact impedance to be  $\approx 70 - 700i$  k $\Omega$  at 10 Hz through two-wire measurements. We use a 300 ms  
82 time constant on the lock-in amplifier and digitally sample the data from the lock-in at a rate of 6 Hz. When we focus on  
83 the long-term behavior of the resistance (e.g., growth or antibiotic susceptibility measurements over two hours), we further  
84 integrate (average) the data numerically over one-minute intervals. When we focus on the short-time fluctuations (i.e., Fig. 4  
85 in main text), we high-pass filter the data using a cut-off frequency of 0.01 Hz.

86 The time-dependent resistance of the device can be expressed as  $R(t) = R_{em} + \Delta R(t)$ , where  $R_{em}$  is the initial resistance  
87 of the microchannels with pure LB broth and  $\Delta R(t)$  is the resistance change induced by bacteria in the microchannels. We  
88 can estimate the minimum detectable  $\Delta R$  from noise analysis. In the experiments, the equivalent noise bandwidth at a time  
89 constant of 300 ms is  $\Delta f \approx 0.31$  Hz (time constant 300 ms and filter roll-off of 18 dB/oct). To determine the experimental noise  
90 floor, we perform a noise measurement using a 3.2 M $\Omega$  source resistor. We obtain a total noise of  $\sim 600$  nV/Hz $^{1/2}$ . This value  
91 is slightly larger than the theoretical value of  $\sim 300$  nV/Hz $^{1/2}$ , obtained from combining the Johnson noise of a 3.2 M $\Omega$  resistor  
92 (230 nV/Hz $^{1/2}$ ) with the input noise,  $V_n^{(a)}$ , of the lock-in at 10 Hz ( $V_n^{(a)} \lesssim 200$  nV/Hz $^{1/2}$ ). We use a low-sensitivity setting on  
93 the lock-in to be able to track the large changes in the device resistance during bacteria growth. The minimum detectable  
94 resistance change or the resistance noise can be estimated from a simple circuit analysis. Here, we assume that the minimum  
95 detectable resistance change (under the imposed current of 10 nA across the device and the lock-in input) results in a voltage  
96 equal to the noise voltage. This provides  $\approx 200$   $\Omega$ , which is close to the resistance fluctuations (noise) observed in LB broth.

97 In order to quantify the effect of the long-term electrical drifts on the sensitivity, we have performed a set of experiments  
98 using devices clogged with 1- $\mu$ m-diameter polystyrene (PS) microspheres. This is similar to clogging the microchannels with  
99 bacteria but, since the PS microspheres do not change in size over time, we are able to extract the electrical drift under  
100 conditions comparable to bacteria experiments. In particular, we clog the devices to resistance values  $R(0)$  (or  $\Delta R(0)$ ) close to  
101 those in bacteria experiments, indicating similar flow rates and initial conditions. Three baseline resistance drifts measured  
102 over the course of 2 hours are shown in Fig. S2A. Since the drift appears linear, we fit it as  $\Delta R(t) - \Delta R(0) \approx -0.26t$  (in units  
103 of k $\Omega$  when  $t$  is in minutes). In an effort to quantify the drift effect on the antibiotic susceptibility tests, we have recalculated  
104 the drift-corrected growth rates (dashed lines in Fig. S2B-F). Here, the solid lines are the results from Fig. 3 in the main text.  
105 In the recalculation, we first subtracted the drift from each data trace and then computed the growth rate. Our conclusion,  
106 after comparing the growth rates of corrected and raw data in Table S2, is that drift can safely be neglected at this stage of  
107 development.

108 **Resistance Change Per Added Bacterium.** We show the resistance change  $\Delta R$  as a function of the number  $n$  of bacteria in  
109 the microchannels for *K. pneumoniae*, *E. coli*, and *S. saprophyticus* in Fig. S3. Data shown in each figure are from three  
110 independent experiments. Red dashed lines are the linear fits to the data. We obtain  $\Delta R_1^{(KP)} \approx 2.5 \pm 0.3$  k $\Omega$  for *K. pneumoniae*  
111 (Fig. S3A),  $\Delta R_1^{(EC)} \approx 3.7 \pm 0.3$  k $\Omega$  for *E. coli* (Fig. S3B), and  $\Delta R_1^{(SS)} \approx 3.5 \pm 1.1$  k $\Omega$  per *S. saprophyticus* (Fig. S3C). The  
112 larger error in *S. saprophyticus* originates from the fact that it is more challenging to count single cells from microscope images  
113 and cells tend to cluster more.

114 The measured  $R_{em}$  is the equivalent resistance of ten parallel microchannels at the center of the microfluidic device:  
115  $R_{em} = \frac{1}{10} R_{em}^{(s)}$ , where  $R_{em}^{(s)}$  is the single microchannel resistance,  $R_{em}^{(s)} = \rho \frac{l}{A}$ , with  $\rho$  being the electrical resistivity of the liquid  
116 media (e.g., LB broth) filling the microchannel,  $l$  and  $A$  being respectively the length and cross-sectional area of the single  
117 microchannel. We assume that the electrical resistance of bacteria is large compared to the media. Thus, the resistance  
118 of a single microchannel with one trapped bacterium can be estimated as  $R_{em}^{(s)} + \Delta R_1^{(s)} \approx \rho \left[ \frac{l-l_B}{A} + \frac{l_B}{A-A_B} \right]$ , where  $l_B$  and  
119  $A_B$  are the length and cross-sectional area of a bacterium, respectively. Here,  $R_{em} \approx 3$  M $\Omega$  in LB broth, which, using the  
120 nominal channel dimensions, gives  $\rho \approx 1.2$   $\Omega \cdot$  m. *K. pneumoniae* is rod-shaped, with  $l_B = 2$   $\mu$ m and  $A_B = 0.8$   $\mu$ m $^2$  (3). Using  
121 these numbers, we obtain  $\Delta R_1^{(s)} \approx 150$  k $\Omega$ . Calculating the equivalent resistance, we find the total resistance change per  
122 bacterium becomes  $\Delta R_1 \approx \frac{\Delta R_1^{(s)}}{100} \approx 1.5$  k $\Omega$ . Note that the resistance change per bacterium very much depends on the size of  
123 the bacterium and how the bacterium blocks the microchannel during growth. It is thus different for *S. saprophyticus* and *E.*  
124 *coli*.

125 **Bacteria Accumulation or Growth Outside of the Microchannels.** We occasionally observe bacteria accumulation outside of the  
126 microchannels or growth outward. Fig. S4 shows two different non-ideal ways bacteria accumulate in the device. The linear  
127 dimensions of the regions immediately upstream and downstream from the microchannels are  $l \times w \times h \approx 75 \times 80 \times 2$   $\mu$ m $^3$ .  
128 The microscope images in Fig. S4 show a portion of this region in addition to the central microchannels. Fig. S4A shows that  
129 bacteria (*E. coli*) can get immobilized in the inlet region; in addition, any bacteria that escapes through the nanoconstriction

130 can proliferate in the outlet region. Fig. S4B shows that bacteria (*S. saprophyticus*) can get stuck at the entry region of the  
 131 microchannels, blocking further bacteria trapping in the microchannels. When bacteria are trapped in these bigger channels  
 132 ( $l \times w \times h \approx 75 \times 80 \times 2 \mu\text{m}^3$ ), the resistance change per added bacterium no longer follows the ideal case discussed in the  
 133 main text. In fact from geometry, the resistance change per bacterium is  $\sim \frac{1}{20} \Delta R_1$ , where  $\Delta R_1 \approx 1.5 \text{ k}\Omega$  is the resistance  
 134 change per added bacterium into one of the ten smaller microchannels, as discussed above. For bacteria accumulating outside  
 135 of this 2- $\mu\text{m}$ -high region, the resistance change is even smaller. Thus, our measured resistance signals mainly come from the  
 136 ten smaller microchannels. We note that bacteria trapped outside the microchannels also grow (or die). Thus, their signals are  
 137 coherently added to the signals developing in the microchannels. Finally, if the experiment continues for a long time, bacteria,  
 138 especially motile strains, tend to escape more readily and/or grow outward after filling the microchannels.

139 **Estimation of Bacterial Doubling Time.** We have estimated the doubling time  $t_d$  of bacteria using resistance change data during  
 140 growth. As discussed in the main text,  $\frac{\Delta R(t)}{\Delta R(0)} \approx \frac{n(t)}{n(0)} = e^{\frac{\ln 2}{t_d} t}$ . Thus,  $t_d$  can be obtained by a linear fit to the natural logarithm of  
 141  $\frac{\Delta R(t)}{\Delta R(0)}$ . Fig. S5 shows a number of fits (dashed lines) to the experimental resistance data (solid lines) for *E. coli*, *K. pneumoniae*,  
 142 and *S. saprophyticus*. Each curve is from an independent experiment. The  $t_d$  and  $R^2$  values are as indicated in the figure.

143 **Data from All Measurements.** Fig. S6 shows the resistance change,  $\Delta R(t) - \Delta R(0) = R(t) - R(0)$ , measured over the course of  
 144 2 hours after sample loading in all our antibiotic susceptibility tests and growth experiments. For each data plot, the right  $y$   
 145 axis shows the change in the number of bacteria in the device,  $\Delta n(t)$ , which is estimated from  $\Delta n(t) = \frac{\Delta R(t) - \Delta R(0)}{\Delta R_1}$  with  $\Delta R_1$   
 146 being the calibration value from Fig. S3. The initial resistances  $R(0)$  measured at the start of each electrical measurement  
 147 are shown in Table S3. The approximate number of trapped bacteria in the microchannels at the start of each electrical  
 148 measurement from microscope images are listed in Table S4.

149 **Metric for Assessing Antibiotic Susceptibility.** A simple metric for aility can be obtained from the time derivative of the  
 150 resistance data,  $\frac{d}{dt} \ln \left[ \frac{\Delta R(t)}{\Delta R(0)} \right]$ . Given that  $\frac{\Delta R(t)}{\Delta R(0)} \approx \frac{n(t)}{n(0)}$  and  $n(t) \approx n(0)e^{rt}$ ,  $\frac{d}{dt} \ln \left[ \frac{\Delta R(t)}{\Delta R(0)} \right] \approx r$ . If  $r > 0$ , the population grows;  
 151 if  $r \leq 0$ , the population does *not* grow. Since  $r$  itself is a function of time, especially for antibiotics acting with some delay, it  
 152 may be more appropriate to consider  $r$  averaged over roughly the second half of the experiment. Thus, we calculate  $\bar{r}$  averaged  
 153 over the last 40 mins of available data, which corresponds to the last 60 mins of the resistance measurement due to the 20-min  
 154 time window of the derivative. Table S2 shows  $\bar{r}$  values in all experiments calculated from raw data as well as drift-corrected  
 155 data (Fig. S2B-F). This metric provides conclusions consistent with standard AST results. We note, however, that  $\bar{r} \leq 0$  may  
 156 be too restrictive a condition for susceptibility, especially for a clinical application. More data and error analysis may allow us  
 157 to relax this condition to  $\bar{r} \leq \varepsilon$ , where  $\varepsilon > 0$ .

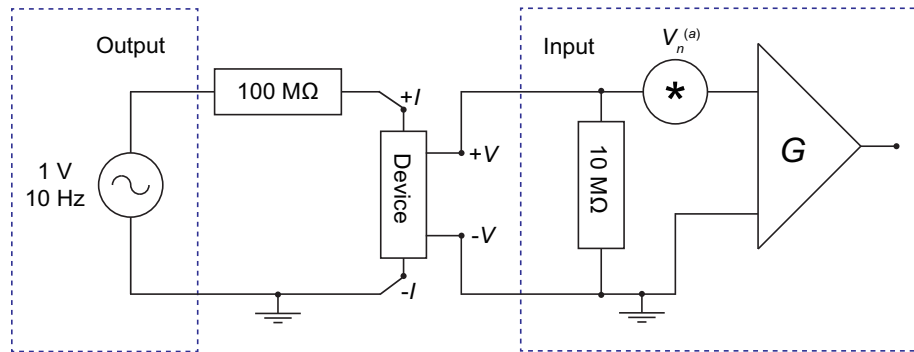


**Fig. S1.** Equivalent-electrical circuit for the measurement. The dashed boxes represent the lock-in amplifier;  $V_n^{(a)}$  is the input noise voltage and  $G$  is the gain of the lock-in amplifier.

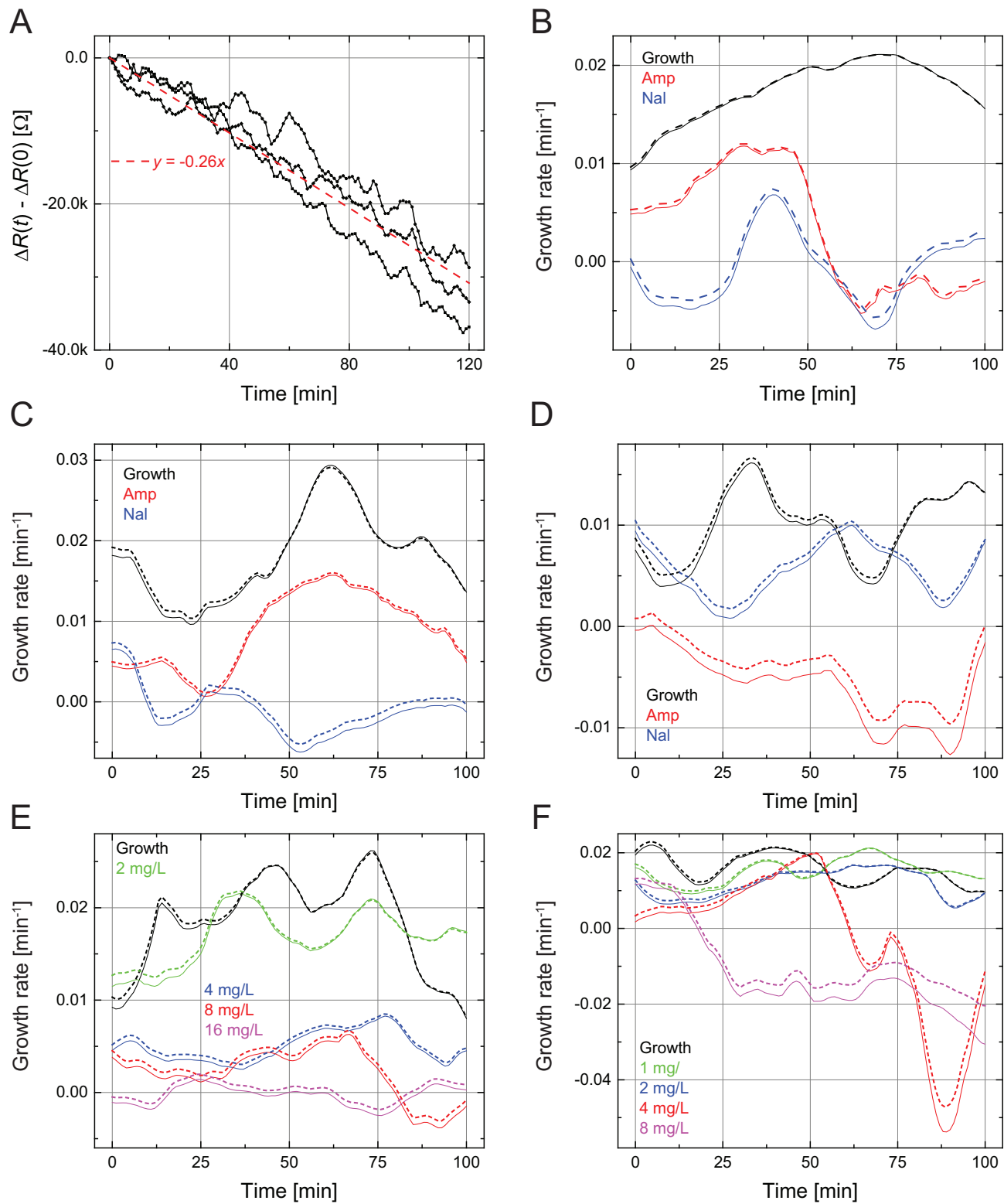


**Fig. S2.** (A) Baseline drifts as a function of time in three independent experiments; the red dashed line shows the linear fit. (B-F) Growth rates from raw (solid lines) and drift-corrected resistance data (dashed lines). Solid lines are reproduced from Fig. 3 in the main text.

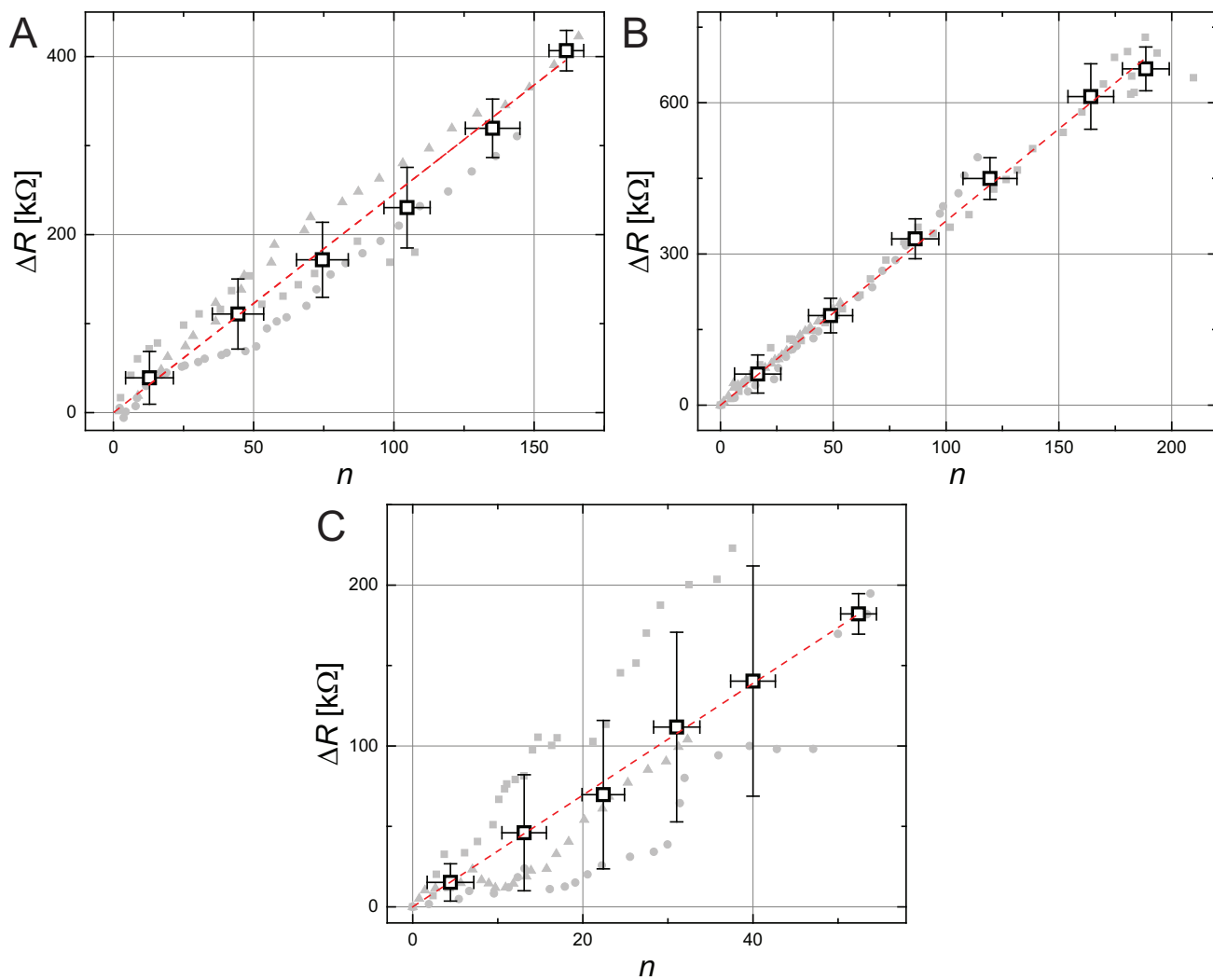


**Fig. S3.** Resistance change  $\Delta R$  as a function of the number  $n$  of bacteria in the microchannels from three independent experiments. (A) *K. pneumoniae*. (B) *E. coli*. (C) *S. saprophyticus*. The red dashed line in each figure shows the linear fit.



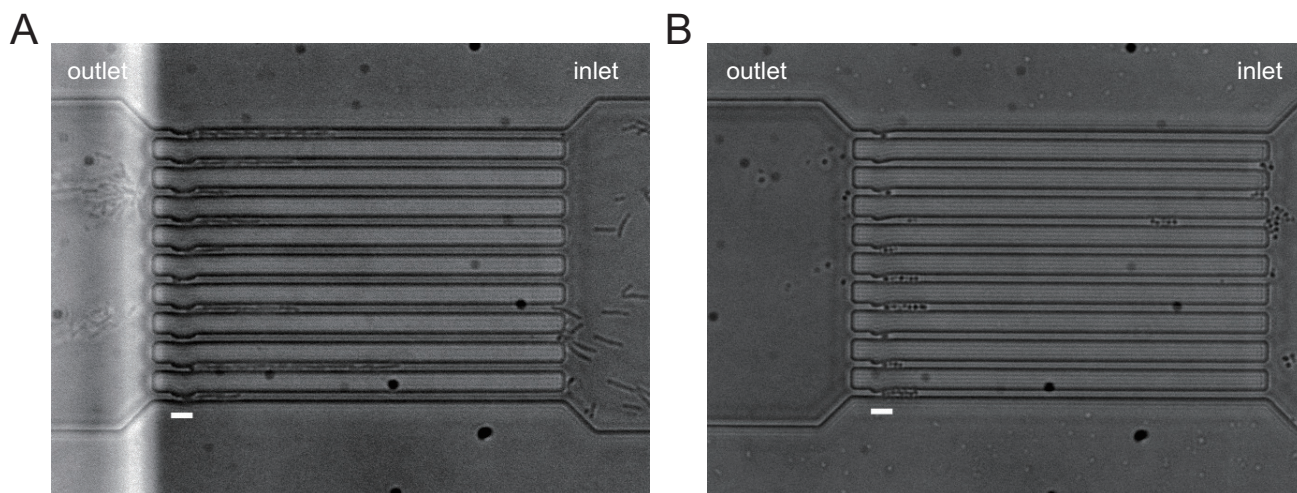


**Fig. S4.** Microscope snapshots showing bacteria accumulation outside the microchannels. (A) *E. coli* (ATCC 25922) growing in LB broth in nalidixic acid (20 mg/L). The bacteria that escaped through the nanoconstriction have proliferated in the outlet region. (B) *S. saprophyticus* (ATCC 15305) growing in LB broth in ampicillin (10 mg/L). Some cells have accumulated at the entry regions of the microchannels. The scale bars are 5  $\mu\text{m}$ .



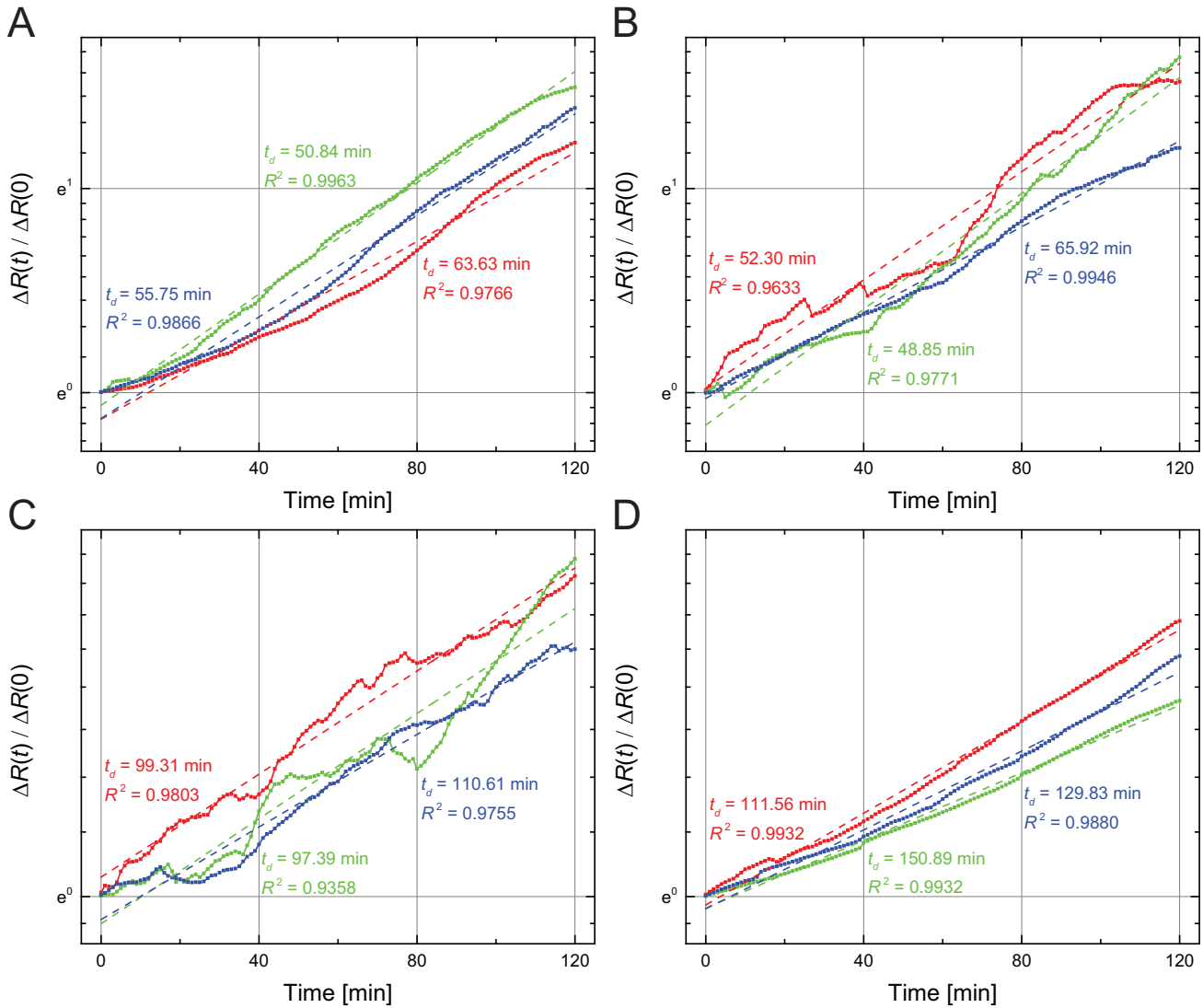


**Fig. S5.** Linear fits to the natural logarithm of  $\frac{\Delta R(t)}{\Delta R(0)}$  in order to determine the bacterial doubling time in the microchannels. (A) *E. coli* (ATCC 25922) at 37 °C. (B) *K. pneumoniae* (ATCC 13883) at 37 °C. (C) *S. saprophyticus* (ATCC 15305) at 37 °C. (D) *E. coli* (ATCC 25922) at 23 °C. Solid lines show data from independent experiments; the dashed lines show the linear fits.

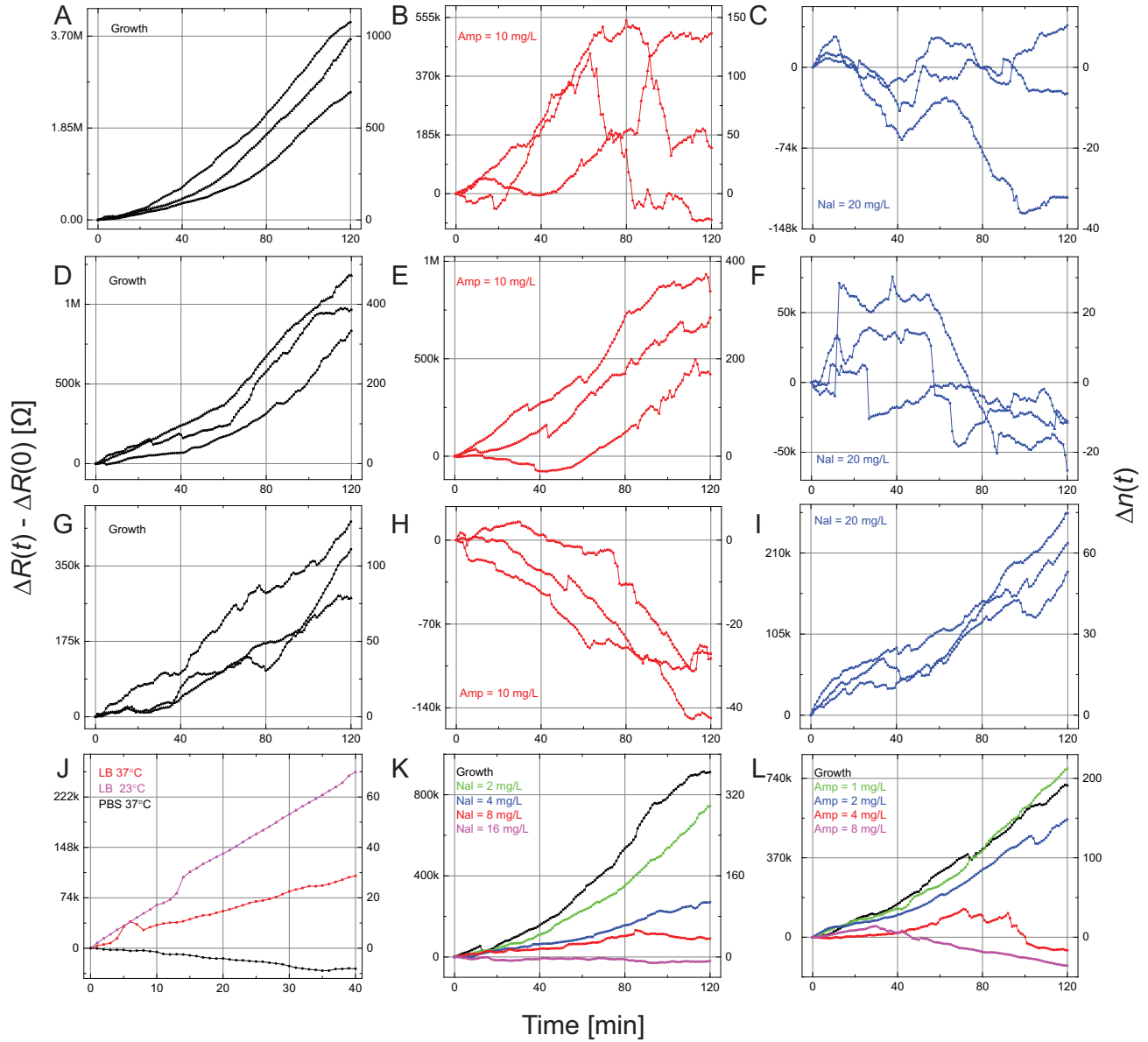


**Fig. S6.** Measured resistance change  $\Delta R(t) - \Delta R(0)$  and change in the number of bacteria,  $\Delta n(t)$ , in the microchannels after sample loading as a function of time. Measurements on *E. coli* (ATCC 25922) (A-C), *K. pneumoniae* (ATCC 13883) (D-F), *S. saprophyticus* (ATCC 15305) (G-I). (J) Measurements on *E. coli* (ATCC 25922) in PBS at 37°C and LB broth at 23°C and 37°C. (K) Measurements on *K. pneumoniae* (ATCC 13883) growing in urine with nalidixic acid at different concentrations. (L) Measurement on *E. coli* (JW 1908-1) growing in urine with ampicillin at different concentrations. Each curve represents one independent experiment.

**Table S1. Summary of MICs of ampicillin and nalidixic acid for *E. coli*, *K. pneumoniae* and *S. saprophyticus* obtained by resazurin-based broth multidilution AST. Results obtained in urine are shown in parentheses.**

Bacteria	Ampicillin (mg/L)	Nalidixic acid (mg/L)
<i>E. coli</i> (ATCC 25922)	8	4-8
<i>K. pneumoniae</i> (ATCC 13883)	> 128	16 (8)
<i>S. saprophyticus</i> (ATCC 15305)	< 0.25	> 128
<i>E. coli</i> (JW 1908-1)	(4)	-

**Table S2. Average growth rates  $\bar{r}$  for all experiments without and with drift correction. Where available, both the average values and the results of individual experiments (in parentheses) are tabulated.**

Bacteria	Antibiotic	Expectation	$\bar{r}$ (min <sup>-1</sup> )	Drift-corr. $\bar{r}$ (min <sup>-1</sup> )
<i>E. coli</i>	Growth (LB)	-	0.019 (0.021, 0.018, 0.019)	0.019 (0.021, 0.018, 0.019)
<i>E. coli</i>	Ampicillin, 10 mg/L	Susceptible	-0.0037 (-0.0005, -0.0099, -0.0006)	-0.0027 (0.0003, -0.0093, 0.0008)
<i>E. coli</i>	Nalidixic acid, 20 mg/L	Susceptible	-0.0017 (-0.0011, 0.0012, -0.0052)	-0.0008 (-0.0005, 0.0023, -0.0043)
<i>K. pneumoniae</i>	Growth (LB)	-	0.021 (0.022, 0.026, 0.015)	0.021 (0.022, 0.026, 0.015)
<i>K. pneumoniae</i>	Ampicillin, 10 mg/L	Resistant	0.0114 (0.0096, 0.0176, 0.0070)	0.0118 (0.0099, 0.0184, 0.0071)
<i>K. pneumoniae</i>	Nalidixic acid, 20 mg/L	Susceptible	-0.0019 (-0.0044, 0.0013, -0.0027)	-0.0010 (-0.0034, 0.0019, -0.0014)
<i>S. saprophyticus</i>	Growth (LB)	-	0.010 (0.007, 0.015, 0.009)	0.010 (0.007, 0.015, 0.009)
<i>S. saprophyticus</i>	Ampicillin, 10 mg/L	Susceptible	-0.0096 (-0.0058, -0.0068, -0.0161)	-0.0071 (-0.0039, -0.0051, -0.0124)
<i>S. saprophyticus</i>	Nalidixic acid, 20 mg/L	Resistant	0.0059 (0.0052, 0.0055, 0.0069)	0.0064 (0.0057, 0.0062, 0.0072)
<i>K. pneumoniae</i>	Growth (urine)	-	0.018	0.018
<i>K. pneumoniae</i>	Nalidixic acid, 2 mg/L	Resistant	0.018	0.018
<i>K. pneumoniae</i>	Nalidixic acid, 4 mg/L	Resistant	0.0059	0.0062
<i>K. pneumoniae</i>	Nalidixic acid, 8 mg/L	Resistant	0.0006	0.0012
<i>K. pneumoniae</i>	Nalidixic acid, 16 mg/L	Susceptible	-0.0008	-0.0002
<i>E. coli</i>	Growth (urine)	-	0.013	0.013
<i>E. coli</i>	Ampicillin, 1 mg/L	Resistant	0.017	0.017
<i>E. coli</i>	Ampicillin, 2 mg/L	Resistant	0.0125	0.0126
<i>E. coli</i>	Ampicillin, 4 mg/L	Susceptible	-0.0232	-0.0197
<i>E. coli</i>	Ampicillin, 8 mg/L	Susceptible	-0.0193	-0.0136

**Table S3. Initial resistances  $R(0)$  for each electrical measurement. Experiments in urine are shown in parentheses.**

Bacteria	Growth (M $\Omega$ )	Ampicillin (M $\Omega$ )	Nalidixic acid (M $\Omega$ )
<i>E. coli</i> ATCC 25922	4.02, 4.10, 4.15	3.47, 3.95, 3.99	3.59, 3.24, 3.59
<i>K. pneumoniae</i> ATCC 13883	3.22, 3.15, 3.46	3.65, 3.47, 3.91	3.41, 3.55, 3.28 (3.24, 3.21, 3.52, 3.45, 3.60)
<i>S. saprophyticus</i> ATCC 15305	3.28, 3.22, 3.24	3.29, 3.37, 3.19	3.28, 3.16, 3.43
<i>E. coli</i> JW 1908-1	-	(3.23, 3.27, 3.26, 3.18, 3.16)	-

**Table S4. Rough number of bacteria trapped in the microchannel region in each experiment as determined from microscope images. Experiments in urine are shown in parentheses.**

Bacteria	Growth	Ampicillin	Nalidixic acid
<i>E. coli</i> (ATCC 25922)	90, 95, 95	70, 95, 95	75, 50, 75
<i>K. pneumoniae</i> (ATCC 13883)	60, 50, 85	85, 65, 95	60, 70, 50 (60, 60, 70, 65, 80)
<i>S. saprophyticus</i> (ATCC 15305)	60, 60, 50	45, 60, 45	40, 50, 65
<i>E. coli</i> (JW 1908-1)	-	(60, 55, 40, 30, 35)	-

158 Movie S1. *E. coli* (ATCC 25922) growth with no drug in the microchannels in LB broth at 37°C. (Left) Time-  
159 lapse imaging showing that the cells are immobilized and growing in the microchannels. Scale bar, 5 μm.  
160 (Right) The normalized electrical resistance change  $\frac{\Delta R(t)}{\Delta R(0)}$  of the microchannels as a function of time. Each  
161 second in the video corresponds to ~ 3 min in the experiment.

162 Movie S2. *E. coli* (ATCC 25922) growth in the presence of ampicillin (10 mg/L) in the microchannels in LB  
163 broth at 37°C. (Left) Time-lapse images show that the trapped cells are elongating and swelling, but do not  
164 divide, and finally burst in the microchannels. Scale bar, 5 μm. (Right) The normalized electrical resistance  
165 change  $\frac{\Delta R(t)}{\Delta R(0)}$  and the resistance fluctuations of the microchannels as a function of time. Each second in the  
166 video corresponds to ~ 3 min in the experiment.

## 167 References

- 168 1. Andrews JM (2001) Determination of minimum inhibitory concentrations. *Journal of antimicrobial Chemotherapy*  
169 48(suppl\_1):5–16.
- 170 2. Wiegand I, Hilpert K, Hancock RE (2008) Agar and broth dilution methods to determine the minimal inhibitory concentration  
171 (mic) of antimicrobial substances. *Nature protocols* 3(2):163.
- 172 3. Berg HC (2008) *E. coli in Motion*. (Springer Science & Business Media).